



Cite this: RSC Adv., 2020, 10, 36818

 Received 19th August 2020  
 Accepted 28th September 2020

 DOI: 10.1039/d0ra07119f  
[rsc.li/rsc-advances](http://rsc.li/rsc-advances)

## 1. Introduction

Regio- and stereo-controlled functionalization of carbon–carbon double bonds has enormous potential in organic synthesis.<sup>1</sup> Allenamides have been widely investigated and utilized as one of the most powerful and versatile building blocks in the field of organic synthesis since the first documentation of their synthesis and characterization in 1968 by Viehe.<sup>2</sup> The  $\pi$ -donating ability of nitrogen atoms renders allenamides more electron-rich than simple alenes, which predisposes them to electrophilic activation. An electronic bias can be exerted through delocalization of the nitrogen lone pair toward the allenic moiety, as demonstrated in the allenamide resonance form. Accordingly, highly regioselective

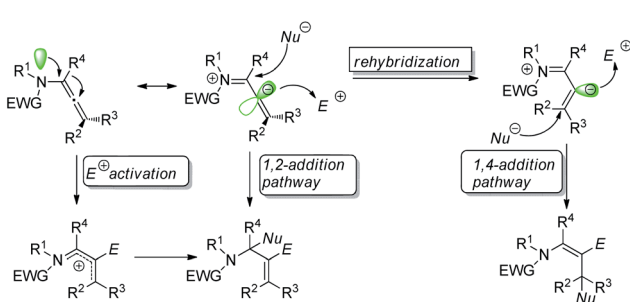
transformations can be achieved by the consecutive addition of electrophiles and nucleophiles (Scheme 1).

With their unique reactivity, selectivity, availability and stability, allenamide functionalization is being increasingly investigated. While a recent review of the flexible reactivity of allenamides in transition-metal-catalyzed functionalization reactions has been published,<sup>3</sup> the present review predominantly summarizes progress in transition-metal-free allenamide functionalization in recent years.

## 2. Chiral phosphoric-acid-catalyzed functionalization of allenamides

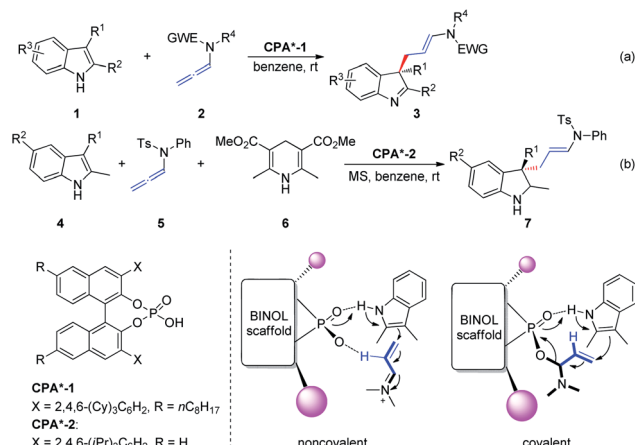
The hydrogen bond activation mode is recognized as one of the most powerful strategies in the field of metal-free asymmetric manipulation of heteroatom-based organic functional groups and anions.<sup>4</sup> Chiral phosphoric acid (CPA)-catalyzed synthesis of value added building blocks, discussed in this section, is continuously expanding within the asymmetric synthesis context.<sup>5</sup>

In 2014, Bandini *et al.*<sup>6</sup> reported the first effective and unprecedented chiral BINOL phosphoric-acid-catalyzed (1–10 mol%) dearomatization of indoles **1** occurring *via* electrophilic activation of allenamides **2** (ee up to 94%). The realization of this transformation resulted in the direct synthesis of densely functionalized enantiomerically enriched 3,3-disubstituted indolene cores **3** featuring an all-carbon quaternary stereogenic center at the C3 position (Scheme 2a). Moreover, the authors extended this methodology to the preparation of enantiomerically enriched 3,3-disubstituted indolines **7** *via* a Brønsted-acid-catalyzed one-pot dearomatization/



Scheme 1 Reaction model of allenamides.

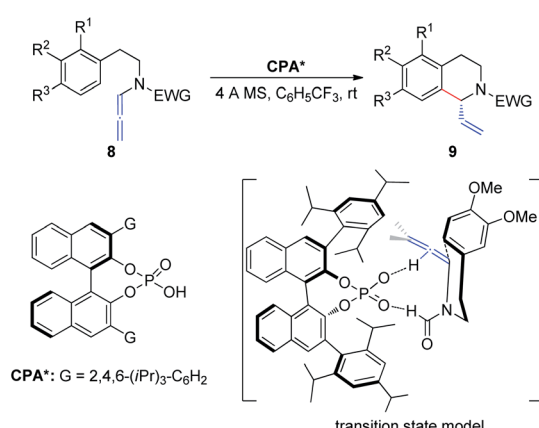




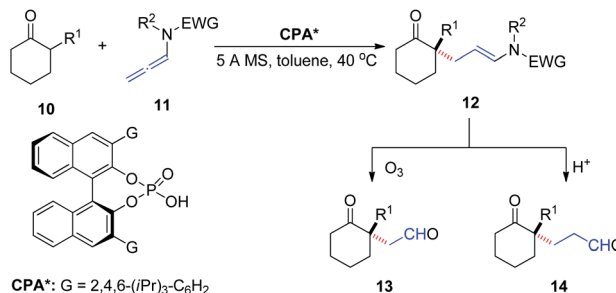
**Scheme 2** Chiral phosphoric-acid-catalyzed asymmetric dearomatization of indoles.

hydrogenation transfer sequence entailing a three-component reaction between indole 4, allenamide 5, and Hantzsch ester 6 (Scheme 2b). The authors proposed two possible activation modes: non-covalent and covalent CPA-allenamide interactions. Subsequently, the reaction mechanism was investigated by means of density functional theory calculations and electrospray ionization mass spectrometry analysis.<sup>7</sup> The first step of the process (rate determining step) was the formation of a covalent adduct between the allenamide and chiral organo-promoter. The resulting chiral  $\alpha$ -amino allylic phosphate undergoes dearomatative condensation with indoles. In the first step, the indole moiety remains bonded to the catalyst through strong hydrogen bonding.

In 2015, Cozzi *et al.*<sup>8</sup> reported the cyclization of allenamides 8 to 1-vinyl tetrahydroisoquinolines 9 in the presence of CPAs (Scheme 3). In this reaction, the elusive and relatively unstable iminium ion derived from acrylaldehyde is generated *in situ* and this electrophilic intermediate can engage in stereoselective intramolecular Friedel-Crafts-type allylic alkylation with electron-rich aromatic rings. In particular, given the importance



**Scheme 3** Chiral phosphoric-acid-catalyzed asymmetric cyclization of allenamides.

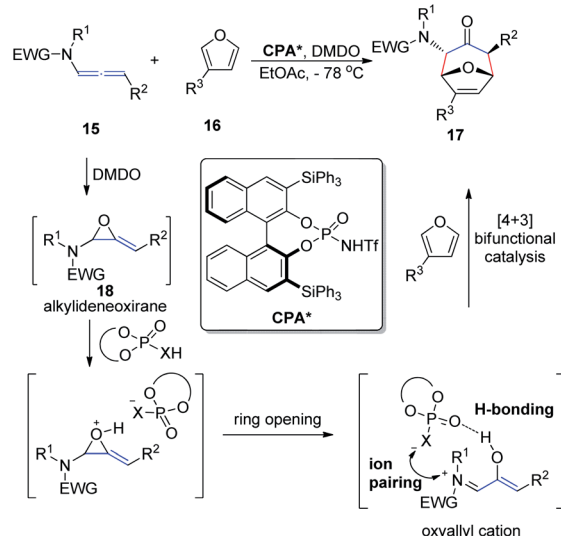


**Scheme 4** Chiral phosphoric-acid-catalyzed asymmetric addition of unactivated  $\alpha$ -branched cyclic ketones to allenamides.

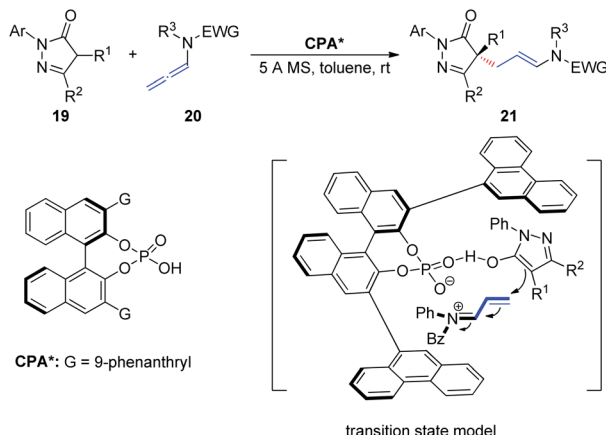
of the formyl group, the authors assumed that the recognition and high enantiomeric excess obtained in the reaction were governed by the hydrogen bonding between the catalyst and the hydrogen atom of the formyl group.

In 2016, Toste *et al.*<sup>9</sup> reported the asymmetric addition of unactivated  $\alpha$ -branched cyclic ketones 10 to allenamides 11 catalyzed by a CPA, to generate an all-carbon quaternary stereocenter 12 with high enantioselectivity (Scheme 4). The reaction exhibited a broad substrate scope, tolerating various aryl, alkenyl, alkynyl, and alkyl substituents as well as cyclohexanone modification. The products could be readily transformed into their corresponding 1,4- and 1,5-ketoaldehyde derivatives 13 and 14, respectively, both of which are important building blocks in organic synthesis.

In 2017, Vicario *et al.*<sup>10</sup> reported that BINOL-based *N*-trifluoromethanesulfonyl phosphoramides catalyze the enantioselective [4 + 3] cycloaddition between furans 16 and oxyallyl cations 18, the latter being generated *in situ* from allenamide 15 oxidation (Scheme 5). This method provides a direct and facile access to a wide range of potentially valuable seven-membered rings 17 in a highly regio-, diastereo-, and enantioselective



**Scheme 5** Enantioselective [4 + 3] cycloaddition catalyzed by chiral *N*-trifluoromethanesulfonyl phosphoramides.

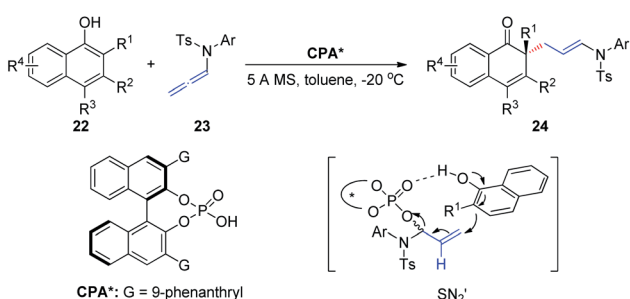


Scheme 6 Chiral phosphoric-acid-catalyzed asymmetric addition of pyrazolones to allenamides.

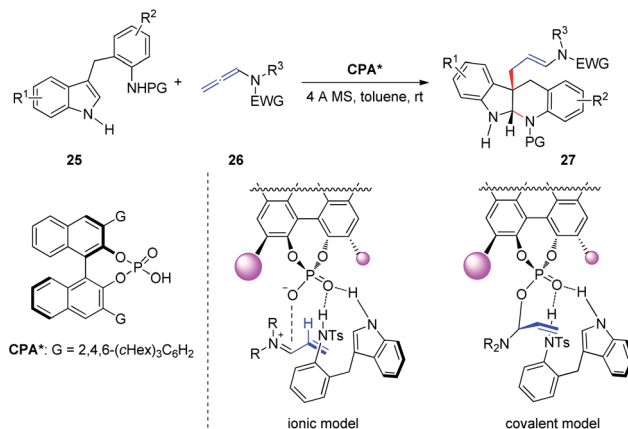
fashion. The reaction relies on the potential of the conjugate base of the *N*-trifluoromethanesulfonyl phosphoramido catalyst to engage in a bifunctional mode of activation, which combines hydrogen bonding with electrostatic interactions by ion pairing with the oxyallyl cation dienophile. This combination enables efficient chirality transfer to the newly formed stereocenters. Moreover, this catalyst system displays a remarkably wide substrate scope with respect to both the furan and allenamide coupling partners, and the excellent performance of  $\gamma$ -substituted allenamides as oxyallyl cation precursors is highlighted.

In 2018, Wang *et al.*<sup>11</sup> described an asymmetric allylic alkylation of pyrazolones *via* CPA-catalyzed asymmetric addition of pyrazolones **19** to allenamides **20** (Scheme 6). The room temperature reaction generates a chiral quaternary stereocenter in high yield and with good enantioselectivity and exhibits a broad substrate scope. Mechanistically, the chiral ion pair generated from protonation of the allenamide by the CPA dictates the enantioinduction of the asymmetric addition process together with an additional hydrogen bonding interaction.

In 2019, Shao *et al.*<sup>12</sup> reported the first chiral phosphoric-acid-catalyzed asymmetric intermolecular C–C bond-forming dearomatization of  $\alpha$ -naphthols **22** (Scheme 7). This method is also applicable to  $\beta$ -naphthols. The transformation proceeds



Scheme 7 Chiral phosphoric-acid-catalyzed asymmetric dearomatization of  $\alpha$ -naphthols.



Scheme 8 Chiral phosphoric-acid-catalyzed asymmetric dearomatic cyclization of homotryptamine derivatives.

with high chemo- and enantioselectivity *via* an allylic substitution reaction and provides enantioenriched  $\alpha$ - and  $\beta$ -naphthalenones bearing an all-carbon quaternary center. Notably, two distinct possible reaction mechanisms can be considered; the first involves a concerted asynchronous  $S_N2$ -like displacement, while the second entails participation of an  $\alpha,\beta$ -unsaturated iminium ion formed upon protonation by the allenamide.

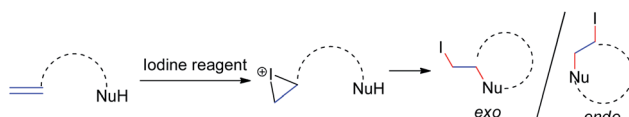
Subsequently, Shin *et al.*<sup>13</sup> reported the CPA-catalyzed asymmetric dearomatic cyclization of homotryptamine derivatives, furnishing enantioenriched indolo[2,3-*b*]quinolone scaffolds **27** in up to 99% ee (Scheme 8). The authors proposed two possible stereochemical models: the basic site of the phosphate in CPA activates homotryptamines **25** *via* dual hydrogen bonding with the indole and aniline in **25**, whereas activation of allenamides **26** by protonation at C2 would form an  $\alpha,\beta$ -unsaturated iminium ion, setting the stage for conjugate addition by the indole moiety of **25** (ionic model). Alternatively, basic phosphate may form a covalent adduct with the iminium to generate an allylphosphate aminal (covalent model), followed by  $S_N2$  attack by the indole C3 carbon. The authors indicated that the covalent model is more favorable than the ionic model based on Bandini's report.<sup>6</sup>

### 3. Iodine-reagent-mediated functionalization of allenamides

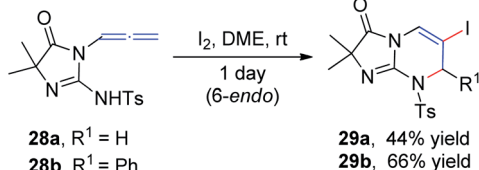
Iodine-containing reagents have received considerable attention as they are inexpensive, nontoxic, and readily available electrophiles that interact with double bonds.<sup>14</sup> The first step in this type of reaction is the interaction between the iodine electrophile and the  $\pi$ -system of the alkene to generate iodiranium intermediates, which subsequently undergo an addition or a cyclization reaction, depending on the stereochemistry and ring size formed, in either *exo* or *endo* fashion, as shown in Scheme 9. This segment reviews recent developments in intramolecular cyclizations and intermolecular nucleophilic additions of allenamides mediated by iodine reagents.

In 1996, Noguchi *et al.*<sup>15</sup> reported the iodine-mediated intramolecular cyclization of *N*-3-allenyl-1-imidazolinones **28**

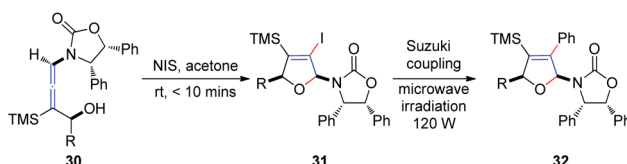




**Scheme 9** The reaction model between iodine electrophiles and carbon–carbon double bonds.



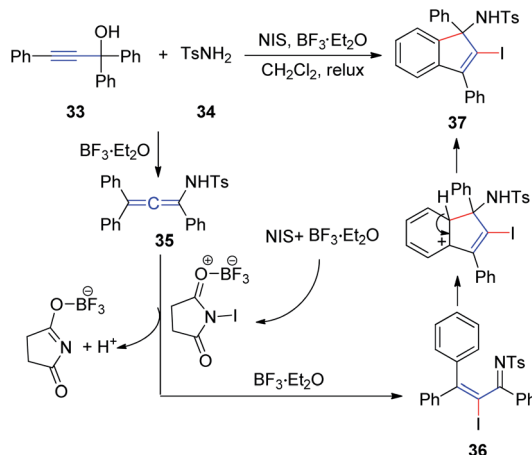
**Scheme 10** Iodine-mediated intramolecular cyclization of 3-allenyl-1-imidazolinones.



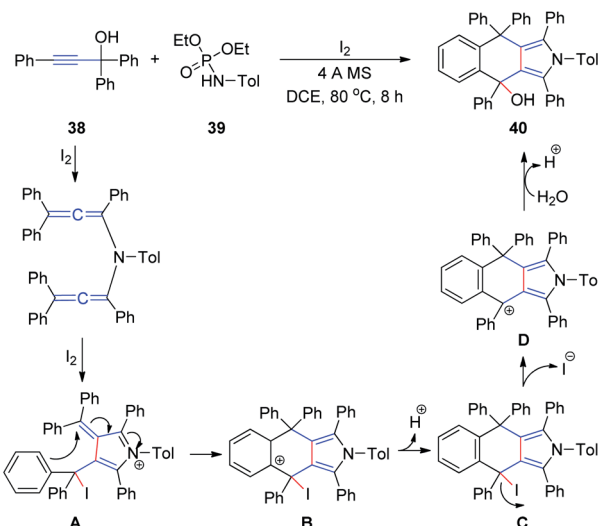
**Scheme 11** *N*-Iodosuccinimide-mediated cyclization of chiral  $\gamma$ -substituted allenamides.

to give 6-*endo* cyclization products **29a** and **29b** in 46% and 66% yields, respectively (Scheme 10).

Subsequently, Hegedus *et al.*<sup>16</sup> developed an *N*-iodosuccinimide-mediated cyclization of chiral  $\gamma$ -substituted allenamides **30**, yielding *cis*-iododihydrofurans **31** with retention of stereochemistry, achieved within 10 min (Scheme 11). The vinyl iodide functionality present in dihydrofurans can be further reacted with phenylboronic acid under Suzuki coupling conditions, providing coupling product **32** in 89% yield under microwave irradiation.



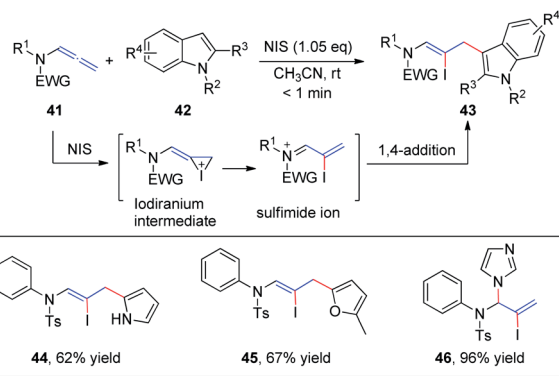
**Scheme 12**  $\text{BF}_3\text{-Et}_2\text{O}$ -catalyzed tandem reaction of propargyl alcohol, sulfonamide, and NIS.



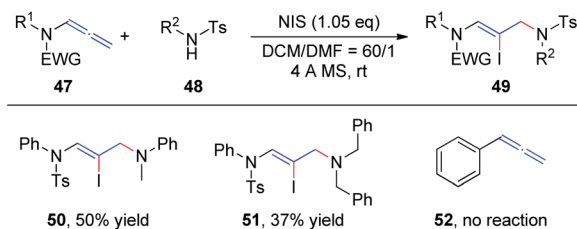
**Scheme 13** Synthesis of 4,9-dihydro-2*H*-benzo[f]isoindoles from propargyl alcohols and phosphoramides in the presence of iodine.

In 2011, Wang *et al.*<sup>17</sup> developed an efficient method to generate *N*-(2-iodoinden-1-yl)arenesulfonamides *via* a  $\text{BF}_3\text{-Et}_2\text{O}$  catalyzed tandem reaction of propargyl alcohol **33**, sulfonamide **34**, and NIS (Scheme 12). Allenesulfonamide **35** is postulated to be a key intermediate for this tandem transformation. Mechanistically, propargyl alcohol and *p*-toluenesulfonamide are first converted to the key allenesulfonamide intermediate under  $\text{BF}_3\text{-Et}_2\text{O}$  catalytic conditions. Meanwhile, in the presence of  $\text{BF}_3\text{-Et}_2\text{O}$ , NIS is activated to an iodonium species, which activates the allenesulfonamide *in situ* to afford  $\alpha$ -iodo- $\alpha$ , $\beta$ -unsaturated sulfonamide **36**. Sulfonamide **36** was subsequently transformed into the final product **37** *via* an intramolecular Friedel-Crafts reaction promoted by  $\text{BF}_3\text{-Et}_2\text{O}$ .

At a later stage, the same group<sup>18</sup> developed a new method for the synthesis of 4,9-dihydro-2*H*-benzo[f]isoindoles **40** from propargyl alcohols **38** and phosphoramides **39** in the presence of iodine in a single step (Scheme 13). First, a diallenamide is formed from propargyl alcohol and phosphoramide in the presence of iodine. Further iodination induces the first



**Scheme 14** NIS-mediated intermolecular iodofunctionalization of allenamides with indoles, pyrrole, and furan.

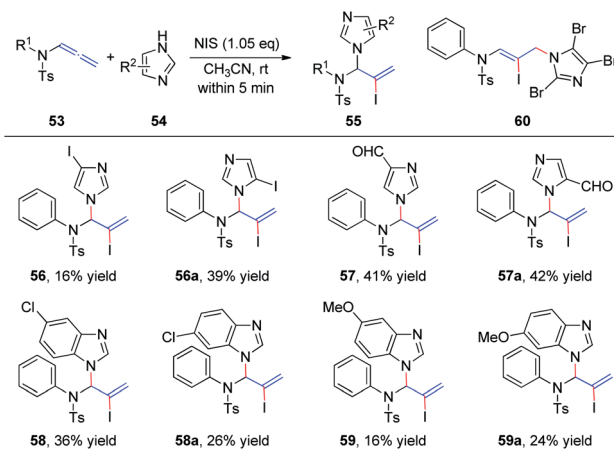


Scheme 15 NIS-mediated iodoamination of allenamides.

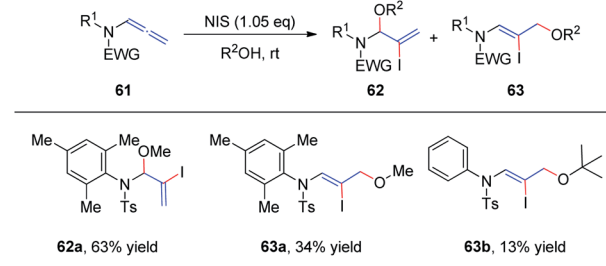
cyclization to give compound **A**. The phenyl ring of **A** then immediately attacks the  $\alpha,\beta$ -unsaturated iminium intramolecularly to execute the second cyclization and deliver **B**. Aromatization of the resulting **C** generates **D**, which is hydrated to afford **40**.

In 2016, our group<sup>19</sup> reported the first *N*-iodosuccinimide-mediated intermolecular iodofunctionalization of allenamides **41** with indoles, pyrroles, and furans, affording the desired 1,4-addition products **43**, **44**, and **45**, respectively, in good yields under mild conditions (Scheme 14). Moreover, when imidazole was used as the nucleophile, the corresponding 1,2-addition product **46** was obtained in good yield. The reaction mechanism involves an iodiranium intermediate, which undergoes a decyclization reaction through the delocalization of the nitrogen lone pair toward the alkene to form the key conjugated sulfimide ion species intermediate. Subsequently, the conjugated sulfimide ion undergoes regioselective addition to give the desired product **43**.

In our preceding report, we found that the degradation product 4-methyl-*N*-phenylbenzenesulfonamide **48** could also be used as a nucleophile to obtain 1,4-addition products, iodine-substituted allylamino *Z*-enamides **49** (Scheme 15). Therefore, we further studied the NIS-mediated iodoamination of allenamides **47** with sulfonamides **48**.<sup>20</sup> These reactions proceed rapidly and tolerate a broad range of substrates. Moreover, *N*-methylaniline and dibenzylamine likewise reacted efficiently with allenamides to obtain the desired products **50** and **51**, respectively, in moderate yields, while unfunctionalized allene **52** could not afford the iodoamination product.



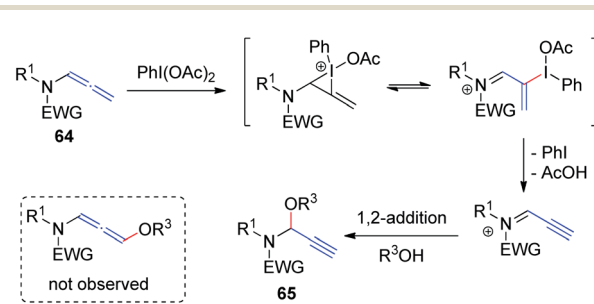
Scheme 16 Regioselective iodoamination of allenamides to generate imidazole heterocycles.

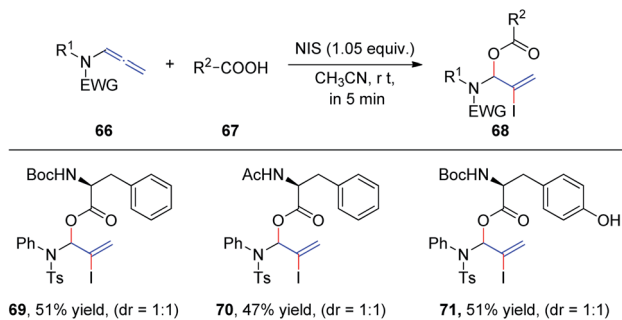
Scheme 17 *N*-Iodosuccinimide-mediated regioselective 1,2-additions of alcohols to allenamides.

and **51**, respectively, in moderate yields, while unfunctionalized allene **52** could not afford the iodoamination product.

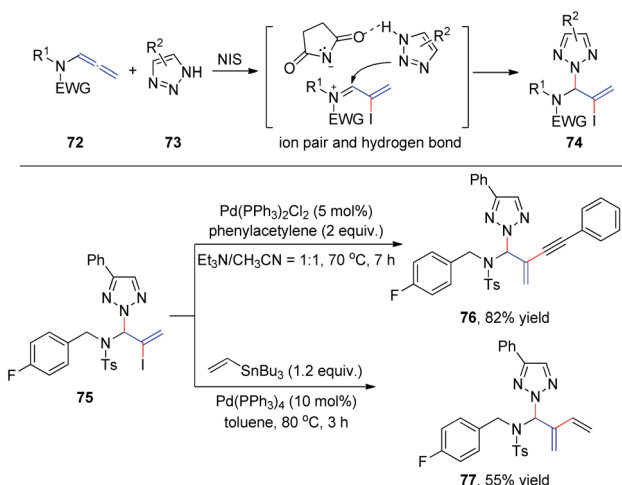
Subsequently, we further extended this regioselective iodoamination of allenamides **53** to imidazole heterocycles **54** (Scheme 16).<sup>21</sup> It is noteworthy that the regioselectivity of this iodoamination appears to differ from that observed in our earlier report<sup>19</sup> involving sulfonamides, to obtain the 1,2-adduct. The facile reaction is regioselective and tolerant of a broad range of imidazole and benzimidazole derivatives. The key intermediate is a conjugated sulfimide ion species that undergoes nucleophilic attack by imidazole to form the 1,2-adduct **55**. Moreover, mixtures of *N*<sup>1</sup>- and *N*<sup>3</sup>-substituted isomers **56/56a**–**59/59a** were obtained using asymmetrically substituted imidazoles, such as 4-iodoimidazole, imidazole-3-carbaldehyde, 5-chloro-1*H*-benzimidazole, and 5-methoxy-1*H*-benzimidazole. In addition, trisubstituted imidazole produced the 1,4-adduct **60** exclusively, because of steric hindrance.

In 2018, we reported the *N*-iodosuccinimide-mediated regioselective 1,2-addition of alcohols to allenamides **61** for the assembly of a series of *N*,*O*-aminals **62** (Scheme 17).<sup>22</sup> These novel reactions proceed rapidly and exhibit a broad substrate scope for a variety of allenamides. It is noteworthy that the alcohol serves as both the solvent and nucleophile in this transformation. Moreover, when trimethylphenyl allenamide was used as the reactant, the 1,2-adduct **62** was obtained in 63% yield, together with the 1,4-adduct **63a** (34% yield); and when *tert*-butanol was employed as the nucleophile and solvent, 1,4-addition product **63b** was isolated in 13% yield as the major product, with both of these experimental results possibly arising from increased steric hindrance.

Scheme 18 Synthesis of propargylic *N*,*O*-acetals via hypervalent iodine-mediated activation of allenamides in alcohols.



Scheme 19 *N*-Iodosuccinimide-mediated intermolecular addition of carboxylic acids to allenamides.



Scheme 20 *N*-Iodosuccinimide mediated  $N^2$ -allylation of triazoles with allenamides.

Yu *et al.*<sup>23</sup> recently demonstrated hypervalent iodine-mediated activation of allenamides **64** in alcohols to obtain propargylic N, O-acetals **65** in high yields with excellent regioselectivity (Scheme 18). By using  $\text{PhI}(\text{OAc})_2$  as the oxidant and an alcohol as both nucleophile and solvent, allenamides were converted to propargylic N, O-acetals **65** *via* 1,2-addition of alcohol to the sulfimide ion intermediate; 1,4-adducts were not detected.

In 2019, we demonstrated the first intermolecular addition of carboxylic acids **67** to the proximal carbon of allenamides **66** toward the regioselective formation of highly useful branched allylic esters **68** by employing *N*-iodosuccinimide (Scheme 19).<sup>24</sup> The reaction proceeded rapidly and displayed a broad substrate scope, providing an efficient and practical protocol for the synthesis of branched allylic esters. Notably, protected amino acids *N*-Boc-*L*-Phe, *N*-Ac-*L*-Phe, and *N*-Boc-*L*-Tyr were tolerated under the reaction conditions and afforded allylic amino acid esters **69**, **70**, and **71**, respectively, in moderate yields and 1 : 1 dr.

Subsequently, we developed a new method for the synthesis of  $N^2$ -allyl-1,2,3-triazoles *via* NIS-mediated allylation of allenamides **72** with mono- and unsubstituted NH-1,2,3-triazoles and

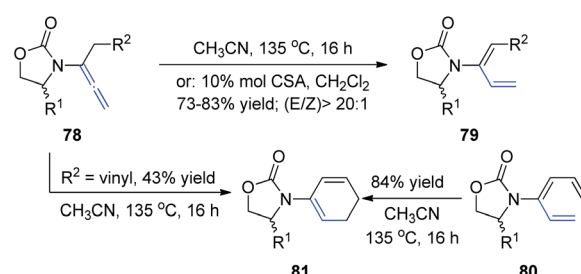
benzotriazole **73** (Scheme 20).<sup>25</sup> The reaction is facile and highly regioselective. The regioselectivity may be induced by the ionic pair composed of a  $\sigma$ -complex and the conjugate base of the imide through hydrogen bonding between the conjugate base and NH-1,2,3-triazole. To further demonstrate the utility of this protocol, product **75** was reacted with phenyl acetylene and vinyl tributylstannane under Sonagashira<sup>26</sup> and Stille<sup>27</sup> cross-coupling conditions, and the corresponding coupling products **76** and **77** were isolated in 82% and 55% yields, respectively.

#### 4. 1,3-H-shift reaction of allenamides

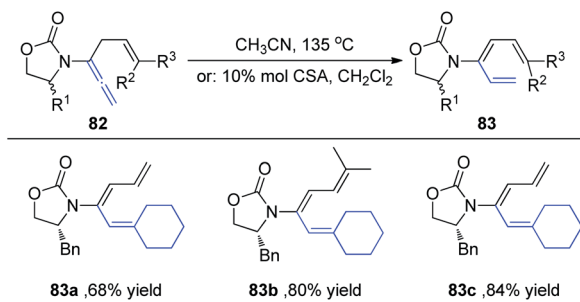
In 2009, Hsung *et al.*<sup>28</sup> described the regio- and stereoselective isomerization of allenamides under thermal or acid-promoted conditions, leading to the preparation of *de novo* 2-amido-dienes and a tandem isomerization-6 $\pi$ -electron electrocyclic ring closure (Scheme 21). This 1,3-H shift was found to be highly regio- and stereoselective, as products **79** were obtained in >20 : 1 *E/Z* ratios. The excellent *E*-selectivity provided a platform for a pericyclic transformation, as allenamide **78** underwent isomerization to give 3-amido-triene **80** in 89% yield. Subsequently, a thermal 6 $\pi$ -electron electrocyclic ring closure of **80** gave cyclic diene **81**. Alternatively, cyclic diene **82** could also be obtained directly from allenamide **80** under thermal conditions in a tandem sequence, albeit in a lower overall yield.

Hsung *et al.*<sup>29</sup> subsequently expanded the substrate scope of the 1,3-H shift reaction for the preparation of 3-amido-trienes **83**. Such 1,3-hydrogen shifts could be achieved thermally or *via* Brønsted acid promotion (Scheme 22). Under either condition, these processes are highly regioselective for the  $\alpha$ -position, and highly stereoselective for the *E*-configuration. For example, when allenamides with both  $\alpha$ - and  $\gamma$ -substitutions were examined, the 1,3-H shift in this case was found to be completely regioselective occurring exclusively from the  $\alpha$ -position to afford highly substituted (*E*)-3-amido-trienes **83a**–**83c** in good yields.

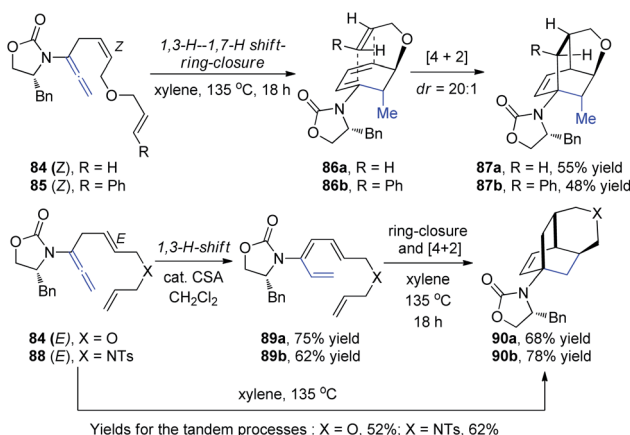
Hsung *et al.*<sup>30</sup> then described a new torquoselective ring closure of chiral amide-substituted 1,3,5-hexatrienes and its application in tandem with [4 + 2] cycloaddition. They found that the reactions of allenamides **84-Z** and **85-Z** led to tricycles **87a** and **87b** as single isomers *via* the highly stereoselective [4 + 2] cycloaddition of cyclic amido dienes **86a** and **86b**, respectively, thereby constituting a quadruple tandem process



Scheme 21 Synthesis of 2-amido-dienes *via* 1,3-H-shift of allenamides.

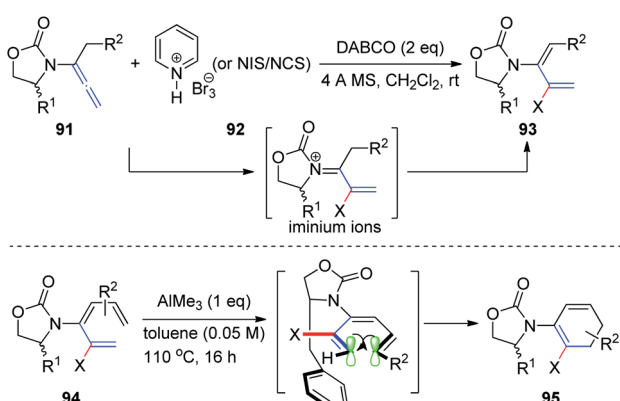


Scheme 22 The synthesis of 3-amido-trienes through 1,3-H-shift of allenamides.

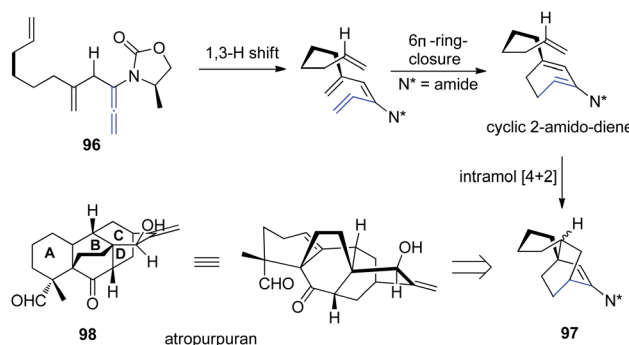


Scheme 23 The tandem process of 1,3-H-1,7-H shift-6 $\pi$ -electron pericyclic ring-closure-[4 + 2] cycloaddition.

entailing a 1,3-H-1,7-H shift-6 $\pi$ -electron pericyclic ring-closure-[4 + 2] cycloaddition. In contrast, reactions of allenamides 84-E and 88-E led to tricycles 90a and 90b in excellent yields and high diastereoselectivity proceeding from amidotrienes 89a and 89b, respectively, or directly from the allenamides in a triple tandem process (Scheme 23). These tandem processes provide a rapid assembly of complex tricycles from very simple allenamides,



Scheme 24 Synthesis of 2-halo-3-amidodi- and -trienes via electrophilic halogenation of allenamides.



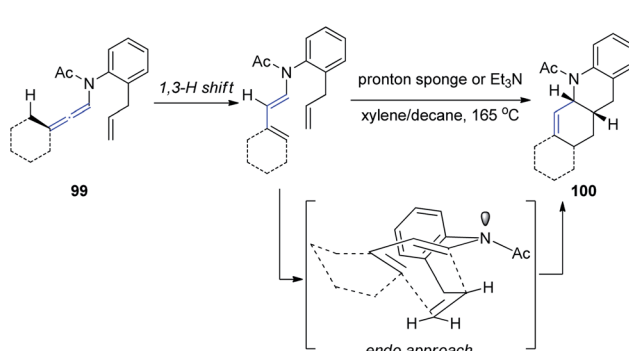
Scheme 25 Synthesis of BCD-ring of atropurpuran via a 1,3-hydrogen shift, 6 $\pi$ -electron pericyclic ring closure, and an intramolecular Diels–Alder cycloaddition.

thereby demonstrating their tremendous power and synthetic potential.

Subsequently, Hsung<sup>31</sup> described a synthetic access to rare 2-halo-3-amidodi- and -trienes 93 via electrophilic halogenation of allenamides 91. These reactions were thought to proceed through the *N*-acyl iminium ion intermediate. Moreover, the successful *de novo* synthesis of chiral 2-halo-3-amidotrienes 94 enabled diastereoselective 6 $\pi$ -electron electrocyclizations *via* a challenging remote 1,6-asymmetric induction with the addition of AlMe<sub>3</sub>. A potential model is presented in Scheme 24 to rationalize the selectivity.

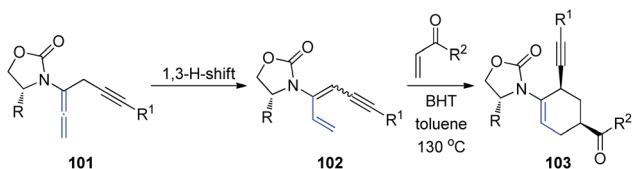
Based on a previous report of a highly stereoselective tandem sequence consisting of an allenic 1,3-hydrogen shift of allenamide 96, followed by 6 $\pi$ -electron pericyclic ring closure, and an intramolecular Diels–Alder cycloaddition, Hsung *et al.*<sup>32</sup> later described an approach toward the BCD-ring of atropurpuran 98 employing this tandem sequence. While the pericyclic ring closure required the assistance of a Lewis acid, the entire process was highly stereoselective for the *endo*-cycloadduct 97 (Scheme 25).

Hsung<sup>33</sup> further developed a new approach to Oppolzer's intramolecular Diels–Alder cycloaddition (IMDA) through the  $\gamma$ -isomerization of readily available *N*-tethered allenamides 99. These IMDA reactions are performed in tandem with the allenamide isomerization or 1,3-H shift, *via* an *endo*-transition



Scheme 26 Oppolzer's intramolecular Diels–Alder cycloaddition via  $\gamma$ -isomerization of allenamides.





Scheme 27 The tandem propargylation-1,3-H-shift sequence of chiral allenamides.

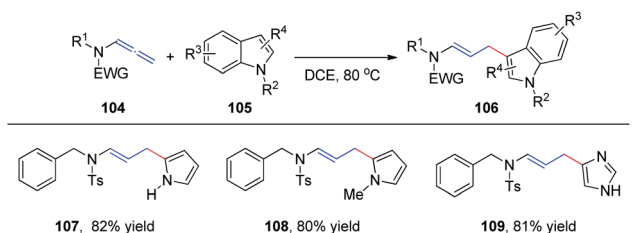
state, as shown in Scheme 26, leading to complex nitrogen heterocycles **100** in a highly stereoselective manner.

Recently, the same group described a tandem propargylation-1,3-H-shift sequence of chiral allenamides **101** to access both *E* and *Z* isomers of chiral 3-amidodienynes (Scheme 27).<sup>34</sup> Moreover, the application of (*Z*)-3-amidodienynes **102** in Diels–Alder cycloadditions gave *endo*-II products **103** in good yields and excellent selectivity, while the reactivity of the corresponding (*E*)-3-amidodienynes toward electrocyclization was inadequate.

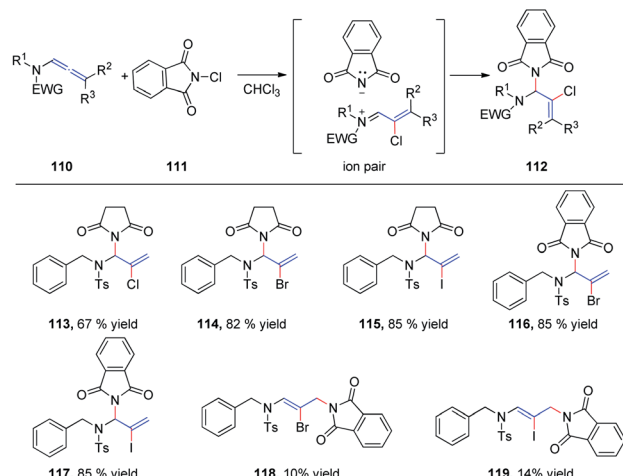
## 5. Other metal-free allenamide functionalization

In 2015, we reported the first catalyst-free intermolecular addition of indoles **105** to the distal double bond of allenamides **104** (Scheme 28).<sup>35</sup> The reaction proceeds smoothly at 80 °C to provide a series of (*E*)-enesulfonamide/enamide derivatives **106** in high yields with excellent regioselectivity. Interestingly, pyrrole, methylpyrrole, and imidazole were likewise efficient nucleophiles, affording the desired products **107**, **108**, and **109** in 82%, 80%, and 81% yields, respectively.

We subsequently reported the regioselective 1,2-addition of allenamides **110** to *N*-chlorophthalimide **111** for the synthesis of 2-chloro allylic aminal derivatives **112** *via* an ion pair composed of a  $\sigma$ -complex and the imide conjugate base (Scheme 29).<sup>36</sup> This reaction was conducted under very mild conditions and afforded yields of up to 99%. *N*-Haloimides served as both electrophiles and nucleophiles in this reaction. Moreover, *N*-chlorosuccinimide, *N*-bromosuccinimide, *N*-iodosuccinimide, *N*-bromophthalimide, and *N*-iodophthalimide were all efficient substrates for the reaction, affording the desired 1,2-adducts **113**–**117** in moderate to good yields. In addition, 1,4-adducts, **118** and **119**, were also isolated when *N*-



Scheme 28 Intermolecular addition of indoles to allenamides under thermal conditions.

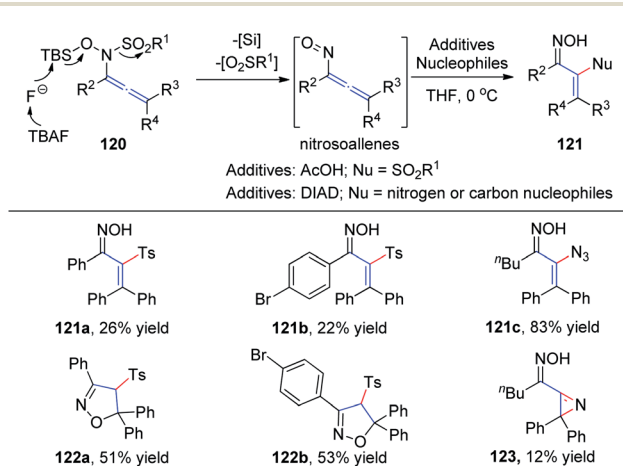


Scheme 29 Intermolecular addition of *N*-chlorophthalimide to allenamides.

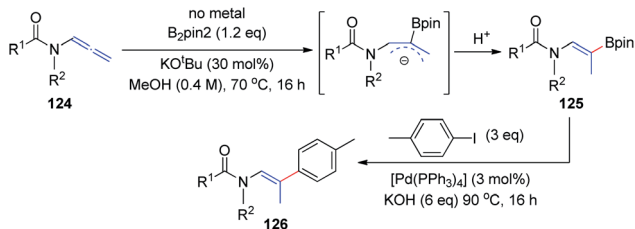
bromophthalimide and *N*-iodophthalimide were used as the reactants.

In 2015, Tanimoto *et al.*<sup>37</sup> developed a synthesis of  $\alpha$ -functionalized enoximes **121** *via* nucleophilic substitution of nitrosoallenes, a novel chemical species prepared from allenyl *N*-hydroxysulfonamides **120** (Scheme 30). Introduction of various nucleophiles proceeded smoothly to create C–N, C–O, C–S, C–F, and C–C bonds in the presence of azodicarboxylates. Interestingly,  $\alpha$ -sulfonyl enoximes **121a** and **121b** were generated *via* sulfone transfer in the presence of AcOH. Moreover, when all the substituents on the allenylamides were aryl groups, 2-isoxazolines **122a** and **122b** were afforded as major products, derived from the cyclocondensation of the initially generated vinylsulfones, likely because of their steric bulkiness. Vinyl azide **121c** was produced in excellent yield as an inseparable mixture with 2*H*-azirine **123**.

In 2018, the Fernández and Vicario group<sup>38</sup> described a high-yielding transition-metal-free borylation of the distal double



Scheme 30 The synthesis of  $\alpha$ -functionalized enoximes *via* nucleophilic substitution of nitrosoallenes.



**Scheme 31** Transition-metal-free borylation of electron-deficient allenamide variants.

bond of electron-deficient variants of allenamides **124**, proceeding with complete stereocontrol to provide *Z* isomers exclusively (Scheme 31). The acyl groups on the amine moiety were crucial for obtaining complete stereoselectivity, owing to the formation of a stable allylic anion intermediate, which is further regioselectively protonated to give the final product **125**. This transition-metal-free borylation can be followed by Pd-catalyzed cross coupling with aryl iodides, to generate trisubstituted olefins **126** in a stereoselective manner.

## 6. Conclusions

Recent advances in transition-metal-free functionalization of allenamides are summarized herein. These innovative transformations have rendered allenamides highly versatile building blocks in organic synthesis, enabling the assembly of a diverse array of carbo- and heterocyclic structures that can serve as platforms for further transformations. Undoubtedly, the level of interest in allenamides from the synthetic community is immensely high, and there is a tremendous momentum to continue developing allenamide methodology and hence expand their synthetic utility.

## Conflicts of interest

There are no conflicts to declare.

## Acknowledgements

This work was financially supported by the Project of Science and Technology Department of Sichuan Province (No. 2018JY0319) and the Fundamental Research Funds of Central Universities, Southwest Minzu University (2020NYB14).

## Notes and references

- (a) X. Wu and L. Z. Gong, *Synthesis*, 2019, **51**, 122–134; (b) D. G. Geng, *Chin. J. Org. Chem.*, 2019, **39**, 301–317; (c) R. Santhoshkumar and C. H. Cheng, *Asian J. Org. Chem.*, 2018, **7**, 1151–1163; (d) H. Hori, S. Arai and A. Nishida, *Adv. Synth. Catal.*, 2017, **359**, 1170–1176; (e) T. Lu, Z. J. Lu, Z. X. Ma, Y. Zhang and R. P. Hsung, *Chem. Rev.*, 2013, **113**, 4862–4904; (f) P. E. Standen and M. C. Kimber, *Curr. Opin. Drug Discovery Dev.*, 2010, **13**, 645–657.
- A. J. Hubert and H. G. Viehe, *J. Chem. Soc. C*, 1968, 228–230.

3 (a) C. Praveen, *Coord. Chem. Rev.*, 2019, **392**, 1–34; (b) J. L. Mascarenas, I. Varela and F. Lopez, *Acc. Chem. Res.*, 2019, **52**, 465–479; (c) E. Manoni and M. Bandini, *Eur. J. Org. Chem.*, 2016, **2016**, 3135–3142; (d) M. E. Muratore, A. Homs, C. Obradors and A. M. Echavarren, *Chem.-Asian J.*, 2014, **9**, 3066–3082; (e) F. Lopez and J. L. Mascarenas, *Beilstein J. Org. Chem.*, 2013, **9**, 2250–2264.

4 (a) *Asymmetric Brønsted Acid Catalysis*, ed. M. Rueping, D. Parmar and E. Sugiono, Wiley-VCH, Weinheim, 2016; (b) Y. L. Yin, X. W. Zhao, B. K. Qiao and Z. Y. Jiang, *Org. Chem. Front.*, 2020, **7**, 1283–1296; (c) M. C. Gimeno and R. P. Herrera, *Eur. J. Org. Chem.*, 2020, **2020**, 1057–1068.

5 (a) V. T. Tran, S. K. Nimmagadda, M. Y. Liu and K. M. Engle, *Org. Biomol. Chem.*, 2020, **18**, 618–637; (b) A. Rahman and X. F. Lin, *Org. Biomol. Chem.*, 2018, **16**, 4753–4777; (c) Y. Kuroda, S. Harada, K. Yamada and K. Takasu, *J. Synth. Org. Chem., Jpn.*, 2018, **76**, 325–335; (d) A. Gualandi, G. Rodeghiero and P. G. Cozzi, *Asian J. Org. Chem.*, 2018, **7**, 1957–1981.

6 C. Romano, M. Q. Jia, M. Monari, E. Manoni and M. Bandini, *Angew. Chem., Int. Ed.*, 2014, **53**, 13854–13857.

7 P. Giacinto, A. Bottone, A. Garelli, G. P. Mischione and M. Bandini, *ChemCatChem*, 2018, **10**, 2442–2449.

8 E. Manoni, A. Gualandi, L. Mengozzi, M. Bandini and P. G. Cozzi, *RSC Adv.*, 2015, **5**, 10546–10550.

9 X. Y. Yang and F. D. Toste, *Chem. Sci.*, 2016, **7**, 2653–2656.

10 L. Villar, U. Uria, J. I. Martinez, L. Prieto, E. Reyes, L. Carrillo and J. L. Vicario, *Angew. Chem., Int. Ed.*, 2017, **56**, 10535–10538.

11 K. Yang, X. Z. Bao, S. Y. Liu, J. N. Xu, J. P. Qu and B. M. Wang, *Eur. J. Org. Chem.*, 2018, **2018**, 6469–6473.

12 B. M. Yang, X. J. Zhai, S. B. Feng, D. Y. Hu, Y. H. Deng and Z. H. Shao, *Org. Lett.*, 2019, **21**, 330–334.

13 S. Biswas, H. Kim, K. L. Cao and S. Shin, *Adv. Synth. Catal.*, 2020, **362**, 1841–1845.

14 (a) S. Hummel and S. F. Kirsch, *Beilstein J. Org. Chem.*, 2011, **7**, 847–859; (b) Y. Yamamoto, I. D. Gridnev, N. T. Patil and T. Jin, *Chem. Commun.*, 2009, **34**, 5075–5087; (c) M. J. Mphahlele, *Molecules*, 2009, **14**, 4814–4837; (d) A. N. French, S. Bissmire and T. Wirth, *Chem. Soc. Rev.*, 2004, **33**, 354–362.

15 M. Noguchi, H. Okada, M. Watanabe, K. Okuda and O. Nakamura, *Tetrahedron*, 1996, **52**, 6581–6590.

16 C. J. T. Hyland and L. S. Hegedus, *J. Org. Chem.*, 2006, **71**, 8658–8660.

17 Y. X. Zhu, G. W. Yin, D. Hong, P. Lu and Y. G. Wang, *Org. Lett.*, 2011, **13**, 1024–1027.

18 G. W. Yin, Y. X. Zhu, L. Zhang, P. Lu and Y. G. Wang, *Org. Lett.*, 2011, **13**, 940–943.

19 H. H. Li, X. X. Li, Z. G. Zhao, T. Ma, C. Y. Sun and B. W. Yang, *Chem. Commun.*, 2016, **52**, 10167–10170.

20 H. H. Li, X. X. Li, Z. G. Zhao, C. B. Lin, T. Ma, C. Y. Sun, B. W. Yang and X. L. Fu, *Tetrahedron Lett.*, 2016, **57**, 4640–4644.

21 Y. Li, G. L. Luo, X. X. Li and Z. G. Zhao, *New J. Chem.*, 2018, **42**, 16940–16947.



22 X. Yuan, X. Man, X. X. Li and Z. G. Zhao, *Tetrahedron*, 2018, **74**, 5674–5682.

23 R. H. Huang, P. Y. Xu, W. X. Wang, G. Peng and H. Yu, *Tetrahedron Lett.*, 2020, **61**, 151753.

24 G. L. Luo, Y. C. Liu, N. Ding, X. X. Li and Z. G. Zhao, *ACS Omega*, 2019, **4**, 15312–15322.

25 X. Man, Y. C. Liu, X. X. Li and Z. G. Zhao, *New J. Chem.*, 2019, **43**, 14739–14746.

26 S. F. Chen, Q. Yan, H. Y. Zhao and B. G. Li, *J. Org. Chem.*, 2013, **78**, 5085–5089.

27 J. L. Stille, *Angew. Chem., Int. Ed.*, 1986, **25**, 508–524.

28 R. Hayashi, R. P. Hsung, J. B. Feltenberger and A. G. Lohse, *Org. Lett.*, 2009, **11**, 2125–2128.

29 R. Hayashi, J. B. Feltenberger, A. G. Lohse, M. C. Walton and R. P. Hsung, *Beilstein J. Org. Chem.*, 2011, **7**, 410–420.

30 R. Hayashi, J. B. Feltenberger and R. P. Hsung, *Org. Lett.*, 2010, **12**, 1152–1155.

31 R. Hayashi, M. C. Walton, R. P. Hsung, J. H. Schwab and X. L. Yu, *Org. Lett.*, 2010, **12**, 5768–5771.

32 R. Hayashi, Z. X. Ma and R. P. Hsung, *Org. Lett.*, 2012, **14**, 252–255.

33 J. B. Feltenberger and R. P. Hsung, *Org. Lett.*, 2011, **13**, 3114–3117.

34 Z. X. Ma, L. C. Fang, B. J. Haugen, D. Bruckbauer, J. B. Feltenberger and R. P. Hsung, *Synlett*, 2017, **28**, 2906–2912.

35 H. H. Li, T. Ma, X. X. Li and Z. G. Zhao, *RSC Adv.*, 2015, **5**, 84044–84047.

36 H. H. Li, X. X. Li, Z. G. Zhao, X. Yuan and C. Y. Sun, *Org. Biomol. Chem.*, 2017, **15**, 4005–4013.

37 H. Tanimoto, K. Yokoyama, Y. Mizutani, T. Shitaoka, T. Morimoto, Y. Nishiyama and K. Kakiuchi, *J. Org. Chem.*, 2016, **81**, 559–574.

38 L. Garcia, J. Sendra, N. Miralles, E. Reyes, J. J. Carbo, J. L. Vicario and E. Fernández, *Chem.-Eur. J.*, 2018, **24**, 14059–14063.

